

Adam S. Davis, PhD^{‡*}
 Thais Federici, PhD^{§*}
 William C. Ray, PhD^{¶||}
 Nicholas M. Boulis, MDS
 Deirdre O'Connor, PhD[§]
 K. Reed Clark, PhD^{‡||#}
 Jeffrey S. Bartlett, PhD^{**}

[‡]Gene Therapy Center and [¶]Battelle Center for Mathematical Medicine, The Research Institute at Nationwide Children's Hospital, Nationwide Children's Hospital, Columbus, Ohio; [§]Department of Neurosurgery, Emory University, Atlanta, Georgia; ^{||}Department of Pediatrics, College of Medicine and Public Health and [#]Department of Molecular Virology, Immunology, and Medical Genetics, College of Medicine and Public Health, The Ohio State University Columbus, Ohio; ^{**}Calimmune, Inc, Tucson, Arizona

*These authors have contributed equally to this article.

Correspondence:

Adam S. Davis, PhD,
 Center for Gene Therapy,
 The Research Institute at Nationwide Children's Hospital,
 700 Children's Drive, W210,
 Columbus, OH 43205.
 E-mail: Adam.
 Davis@NationwideChildrens.org

Received, March 6, 2014.

Accepted, September 26, 2014.

Published Online, December 29, 2014.

Copyright © 2014 by the
 Congress of Neurological Surgeons.



WHAT IS THIS BOX?

A QR Code is a matrix barcode readable by QR scanners, mobile phones with cameras, and smartphones. The QR Code above links to Supplemental Digital Content from this article.

Rational Design and Engineering of a Modified Adeno-Associated Virus (AAV1)-Based Vector System for Enhanced Retrograde Gene Delivery

BACKGROUND: After injection into muscle and peripheral nerves, a variety of viral vectors undergo retrograde transport to lower motor neurons. However, because of its attractive safety profile and durable gene expression, adeno-associated virus (AAV) remains the only vector to have been applied to the human nervous system for the treatment of neurodegenerative disease. Nonetheless, only a very small fraction of intramuscularly injected AAV vector arrives at the spinal cord.

OBJECTIVE: To engineer a novel AAV vector by inserting a neuronal targeting peptide (Tet1), with binding properties similar to those of tetanus toxin, into the AAV1 capsid.

METHODS: Integral to this approach was the use of structure-based design to increase the effectiveness of functional capsid engineering. This approach allowed the optimization of scaffolding regions for effective display of the foreign epitope while minimizing disruption of the native capsid structure. We also validated an approach by which low-titer tropism-modified AAV vectors can be rescued by particle mosaicism with unmodified capsid proteins.

RESULTS: Importantly, our rationally engineered AAV1-based vectors exhibited markedly enhanced transduction of cultured motor neurons, diminished transduction of nontarget cells, and markedly superior retrograde delivery compared with unmodified AAV1 vector.

CONCLUSION: This approach promises a significant advancement in the rational engineering of AAV vectors for diseases of the nervous system and other organs.

KEY WORDS: AAV-mediated gene delivery, Motor neuron disease, Rational design, Retrograde axonal transport, Vector engineering, Vector targeting

Neurosurgery 76:216–225, 2015

DOI: 10.1227/NEU.0000000000000589

www.neurosurgery-online.com

Adeno-associated virus (AAV) has emerged as a promising vector for gene delivery because of its broad-tissue tropism, safety, ability to transduce both quiescent and dividing cells, and ability to mediate long-term gene expression. Recent isolation of novel AAV serotypes and

advances in vector engineering have further enhanced the utility of these vectors. Gene therapy holds a variety of advantages for the treatment of a variety of neurological diseases. In several of these diseases, an optimal therapeutic response is facilitated by vectors that are capable of efficient retrograde axonal transport. In Parkinson disease, preservation and repair of the nigrostriatal pathway may require the expression of trophic genes in both the striatum (postsynaptic) and substantia nigra (presynaptic).¹ This type of targeting is facilitated by the ability of viral vectors to undergo retrograde axonal transport from the postsynaptic site into the presynaptic neurons. Similarly, retrograde transport can facilitate the delivery of genes to target neurons that are widely dispersed as in the case of treating corticospinal neurons to enhance spinal cord regeneration. Finally, retrograde vector

ABBREVIATIONS: AAV, adeno-associated virus; ALS, amyotrophic lateral sclerosis; DMEM, Dulbecco-modified Eagle medium; DRG, dorsal root ganglia; DRP, DNase-resistant particle; MOI, multiplicity of infection; PBS, phosphate-buffered saline; PCR, polymerase chain reaction; rAAV, recombinant adeno-associated virus

Supplemental digital content is available for this article. Direct URL citations appear in the printed text and are provided in the HTML and PDF versions of this article on the journal's Web site (www.neurosurgery-online.com).

delivery provides a minimally invasive means to access neurons in remote or sensitive structures, as is the case for dorsal root ganglia (DRG) in the treatment of neuropathy and pain or spinal cord motor neurons in the treatment of motor neuron diseases. Our laboratory has focused on both idiopathic and genetic motor neuron diseases. However, AAV-mediated retrograde gene delivery to motor neurons remains limited by inefficient axon binding and poor retrograde axonal transport.^{2,3}

Previously, we isolated Tet1, a 12-mer linear peptide that binds selectively to differentiated pheochromocytoma (PC12) cells, primary motor neurons, and DRG in vitro.⁴ We showed that Tet1 binds to the tetanus toxin GT1b receptor and described the in vivo neuronal binding properties and spinal cord uptake of Tet1 after peripheral delivery,⁵ suggesting that insertion of this epitope into the AAV capsid might allow the generation of modified vectors with enhanced axon terminal binding and uptake. Although several studies have demonstrated genetic incorporation of peptide epitopes into the AAV2 capsid and subsequent modification of vector tropism,⁶⁻⁹ our group has defined sites amenable to peptide insertion in other serotype AAV capsids¹⁰ and has demonstrated that these peptide-modified vectors can also transduce target cells via these engineered interactions¹⁰⁻¹³ Because AAV1 vectors have proven superior to AAV2 vectors for neuronal gene delivery and retrograde axonal transport, we sought to modify the AAV1 capsid by Tet1 peptide insertion.² Computational modeling was used to analyze capsid structure and conformation and to visualize and determine the optimal structural context for peptide display. This approach was instrumental in our ability to produce Tet1-modified AAV1 vectors and for these vectors to function properly and direct gene transduction to motor neurons.

Through this work, we have combined the goals and approaches of computational molecular design and capsid structure analysis to provide tools for the rational mutagenesis and functional modification of AAV vector particles. This approach used the analysis of 3-dimensional capsid structure to guide the selection of appropriate amino acid sequences to create a desired property or function. The convergence of high-speed computing, a tremendous increase in capsid structural information, and a growing understanding of the forces that control protein structure and maintain essential viral functions has resulted in dramatic advances in our ability to engineer protein function and structure and to create novel, rationally designed virus-based gene transfer vectors. Such an enhancement in our ability to engineer vectors for specific functions may prove critical to the practical application of gene transfer for a variety of therapeutic paradigms in addition to the studies described here for sensory and motor neuron gene delivery.

METHODS

Construction of Modified AAV Helper Plasmids

Modified AAV1 helper constructs encoding capsid proteins with Tet1 motif insertions were generated by polymerase chain reaction (PCR)-based site-directed mutagenesis as previously described.¹⁰ Briefly, DNA

primers were designed to encode the Tet1 motif and scaffolding sequences (Table) and used to direct PCR-based mutagenesis of the AAV helper plasmid pXR1.^{14,15} This plasmid contains the entire AAV genome, encoding AAV2 Rep proteins and AAV1 Cap proteins, less the 2 viral inverted terminal repeats. PCR products were digested with *DpnI* endonuclease to eliminate the parental plasmid template and were propagated in DH-5a bacteria (Invitrogen Life Technologies, Grand Island, New York). The nonhomologous linker sequences included in the PCR primers to encode the Tet1 scaffolding sequences were also designed to contain restriction sites. Therefore, mini-prep plasmid DNA could be extracted from ampicillin-resistant colonies and screened by restriction endonuclease digestion for confirmation of epitope insertion. Furthermore, all constructs were also subsequently sequenced to confirm epitope insertion and lack of second-site mutations.

Vectors

AAV1eGFP or AAV1RFP (dsRed2) vectors were produced by triple transfection as previously described.¹⁰ To produce AAV vectors comprising Tet1-modified capsid proteins, HEK 293 cells were transfected with modified AAV helper plasmids, constructed as described above, in place of unmodified pXR1. In instances when mosaic particles were generated, unmodified pXR1 was included at a 20% molar equivalent of Tet1-modified AAV helper plasmid as described previously.¹³ Transfections were carried out at 37°C with the use of the calcium phosphate transfection system (Invitrogen Life Technologies) according to the manufacturer's specifications. Forty-eight hours after transfection, cells were harvested by centrifugation at 500g for 10 minutes and resuspended in phosphate-buffered saline (PBS), and vector was released in 3 freeze-thaw cycles. The crude lysate was clarified by centrifugation at 500g 10 minutes, and viscosity was reduced by the addition of Benzonase (250 U/mL) and incubation at 37°C for 30 minutes. Lysate was then fractionated on an iodixanol step gradient¹⁶ and further purified by high-performance liquid chromatography as described previously.¹⁷ Final vector preparations were stored at -20°C in PBS containing 20% glycerol. DNase-resistant particle (DRP) values were determined by real-time PCR assay.¹⁰

Cell Lines

Low-passage-number (passage number 20-40) HEK 293 cells¹⁸ and HeLa C12 cells¹⁹ were grown in Dulbecco-modified Eagle medium (DMEM) supplemented with 10% heat-inactivated fetal bovine serum, penicillin (100 U/mL), and streptomycin (100 U/mL) at 37°C and 5% CO₂. PC12 pheochromocytoma cells were grown in DMEM supplemented with 10% horse serum, 5% fetal bovine serum, and penicillin (100 U/mL). For differentiation, cells were exposed for 2 to 3 days to 100 ng/mL of nerve growth factor (nerve growth factor 2.5S, Invitrogen

TABLE. Summary of Tet1 Insertion Mutants^a

Vector Designation	Upstream Linker	Tet1 Peptide Epitope	Downstream Linker
AAV1.D590_P591insTet1a	AS	HLNILSTLWKYR	GLS
AAV1.D590insTet1b	ASDA	HLNILSTLWKYR	GLS
AAV1.D590_P591insTet1c	ASDA	HLNILSTLWKYR	ADGLS

^aAAV, adeno-associated virus; AS, alanine-serine; GLS, glycine-leucine-serine.

Life Technologies) in DMEM with 2% horse serum and 1% fetal bovine serum. C2C12 cells²⁰ were cultured in Corning 6-well plates (Fisher, 07-200-80) with 1× DMEM (Gibco, 11965-092) supplemented with 10% Hyclone Cosmic Calf Serum (GE, SH30087.04IR) and 10 µg/mL ciprofloxacin.

Primary Cell Cultures

Spinal cords were obtained under sterile conditions from 15-day-old Sprague-Dawley rat embryos following an established protocol.²¹ DRG and perineural membranes were removed, and cords were cut into 2-mm sections, which were then trypsinized. Cells were collected, centrifuged, pelleted, and then resuspended in complete growth medium made in supplemented Neurobasal Medium (Invitrogen Life Technologies). Cells were plated on glass coverslips in multiwell culture plates precoated with poly-L-lysine (Sigma-Aldrich, St. Louis, Missouri).

Campanot Chambers

Campanot Teflon chamber dividers (Tyler Research, Edmonton, Alberta, Canada) were carefully attached to Collagen/Matrigel-coated 35-mm culture dishes using silicone vacuum grease (Dow Corning, Midland, Michigan). Scratches were made in the Collagen/Matrigel with a pin rake. One drop of medium containing methylcellulose (1%) was placed onto the plate before the divider was set on the culture dish, which facilitated axon growth underneath the silicon grease barriers.²² DRG explants were plated into one of the compartments of the chambers in a small volume of media and allowed to adhere for 2 hours. The compartment was then filled with growth medium. The adjacent compartments were filled with media supplemented with 100 ng/mL nerve growth factor to encourage neurite growth into these compartments.

Modeling

Modeling of modified AAV capsid structures was carried out first with SWISS-Model (<http://swissmodel.expasy.org/>)^{23,24} and later with I-TASSER (<http://zhanglab.cmb.med.umich.edu/I-TASSER/>).²⁵⁻²⁷ The capsid protein was initially modeled as a monomer and extended to a trimer after automated modeling. SWISS-Model experienced difficulty in finding adequate loop structures for the Tet1c mutant in the automated mode and generally produced results that did not appear physiologically relevant even when using the alignment mode with a forced alignment to the relevant region of PDB 1LP3. I-TASSER successfully predicted several potential structures for each Tet1 structure with no constraints on the modeling. The SWISS-Model results and the I-TASSER results agreed on the probable structure of the inserted Tet1 sequence itself, including the location of the turn between the antiparallel β sheets. I-TASSER, however, positioned the Tet1 mutant insertions in physiologically realistic locations folded against the surface of the monomer, whereas SWISS-Model preferred to leave the insert as a free strand projecting into space. Although I-TASSER produced several potential results for each mutant, the majority of the structural differences between I-TASSER models were in the predicted structure of the N-terminal region of the protein, quite distant from the insert site. The position of the Tet1 mutants was generally as described in Figure 1, for which we used the highest-confidence I-TASSER-predicted result. The trimeric forms for the structures were constructed by structurally aligning the mutants with PDB 1LP3 and using the capsid-creation rotation symmetry matrices from that file. The trimer was constructed of capsid subunits 0, 19, and 45. Only the Tet1a mutant required manual intervention, inversion of the β-turn curl direction, to avoid physiolog-

ically impossible topological conflicts. To increase our confidence that the folded positioning of the insert sequence was correct, we performed brief (40 000 time step, 2 femtoseconds per step) molecular minimizations of the trimer interface regions using NAMD (Theoretical and Computational Biophysics group at the Beckman Institute, University of Illinois at Urbana-Champaign).²⁸ Although insufficient to predict a lowest-energy conformation, our experience has been that these parameters are sufficient to detect dramatic spatial clashes caused by compositing independently modeled subunits. Each predicted mutant structure experienced some side-chain optimization during the minimization run, but none displayed symptoms of impossibly close van der Waals interactions or other signs of physical implausibility. We therefore believe that the modeled locations of the Tet1 mutants are physiologically reasonable possibilities for their placement.

Immunocytochemistry

Staining was performed with the neuronal cell marker Map-2. The protocol consisted of fixing the cell cultures for 40 minutes with 4% paraformaldehyde in 0.1 mol/L PBS (pH 7.4) and blocking them with 0.1% Triton X-100 to 3% bovine serum albumin in PBS for 1 hour, before an overnight incubation with the primary antibodies. The next day, cells were washed 3 times with 1% bovine serum albumin/PBS and incubated for 1 hour with fluorochrome-conjugated secondary antibodies at room temperature. After washing, the coverslips were mounted on slides using Vectashield Mounting Medium with DAPI (Vector Laboratories, Burlingame, California).

Comparative Gene Transduction Assays

Titer-matched vector solutions (unmodified and Tet1-modified recombinant AAV1 [rAAV1]) were added to cultures and rocked gently to ensure equal distribution of the suspension over the cells. Typically, 3 wells per condition were used. Cells were fixed and processed for analyses 3 days after treatment. Images of transduced cells were acquired with a Nikon E400 microscope using a DS-Qi1 high-sensitivity cooled charge-coupled device camera and analyzed by use of the NIS-Elements imaging software (Nikon Instruments, Inc, Melville, New York) from 10 randomly selected fields per slide. The percentage of green fluorescent protein (GFP)- or red fluorescent protein-positive cells was determined by dividing the number of cell marker-positive, DAPI-positive cells that were also GFP- or red fluorescent protein-positive by the total number of cell marker-positive, DAPI-positive cells. Graphs of the relationship between dose and percentage of transduced cells were then generated. Data were expressed as mean ± SEM.

For quantification of gene transduction in Campanot chambers, the NIS-Elements imaging software was used to compare the fluorescence pixel intensity within the DRG cell bodies. By drawing a region of interest around the explants (white lines), we limited the area that was analyzed. Two channels of fluorescence were captured. The first channel was an internal control to compensate for variability of thickness, size, or density of cells within the explants. It consisted of DAPI staining (see **Figure A, Supplemental Digital Content 1**, <http://links.lww.com/NEU/A693>). The second channel recorded levels of fluorescence resulting from gene expression (see **Figure B, Supplemental Digital Content 1**, <http://links.lww.com/NEU/A693>), which was then expressed as a ratio of the internal control. The software calculated the area of pixel intensity within each region of interest (Table), and a graph was generated.

C2C12 cells at confluence were transduced with either control scrAAV1.eCBA.eGFP vector or scrAAV1tet1.eCBA.eGFP vector at

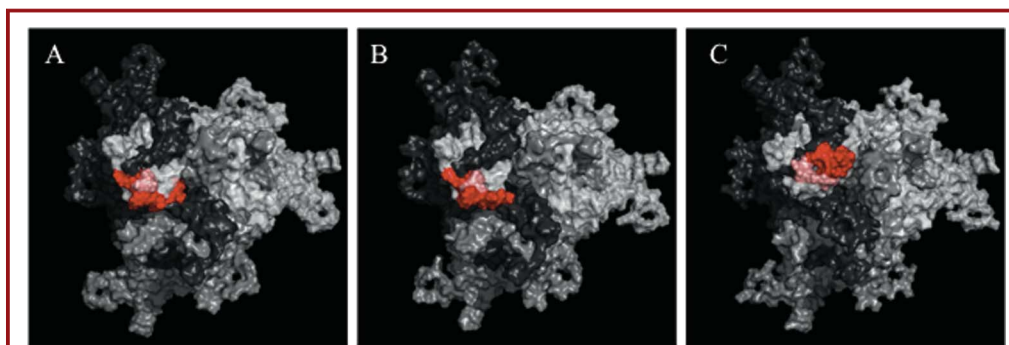


FIGURE 1. A molecular modeling comparison of linker sequence effect on Tet1 peptide display and perturbation of native structure. The adeno-associated virus (AAV) capsid 3-fold axis of symmetry is depicted as a solvent exclusion surface, with each monomer a unique shade of gray, whereas the Tet1 peptide and linker sequences have added van der Waals spheres and are shaded red and pink, respectively. **A.** I-TASSER modeling of Tet1 with C-terminal linker alanine-serine (AS) and N-terminal linker glycine-leucine-serine (GLS; Tet1a) suggests that the peptide folds into the interface between and partially beneath the interlocking arms of each monomer that creates the 3-fold axis of symmetry of capsid. **B.** the C-terminal linker ASDA and N-terminal linker GLS (Tet1b) slightly change the side-chain polarity and presentation geometry of the peptide so that it is more accessible to the capsid exterior; however, it is still partially buried under the capsid surface. **C.** our modeling predicts that the C-terminal linker ASDA and N-terminal linker ADGLS (Tet1c) provide the best opportunity for maximum surface exposure of the Tet1 peptide on the exterior of the capsid with the least disruption of the native capsid structure.

multiplicity of infection (MOI) of 10 000 and 33 000 in serum-free Gibco 1× DMEM. The cells were centrifuged at 1000 rpm for 30 minutes at room temperature and incubated for 4 hours at 37°C and 5% CO₂. At 4 hours after transduction, the wells were spiked to a final concentration of 2% serum and incubated at 37°C and 5% CO₂ for approximately 48 hours. The cells were rinsed with Gibco 1× Hanks balanced salt solution and harvested with Hyclone 0.05% trypsin containing 25 μmol/L EDTA. The trypsin was neutralized with Gibco 1× DMEM containing 10% Hyclone Cosmic Calf Serum and 10 μg/mL ciprofloxacin. The cells were centrifuged at 1000 rpm for 20 minutes and resuspended in Teknova TMN₂₀₀. Cells positive for GFP and mean fluorescence were determined by flow cytometry. Data were collected on a Becton Dickinson LSRII cytometer using BD FACSDiva software. A total of 30 000 events were collected for each sample, and viable cells were gated via a forward-scatter vs side-scatter plot. GFP-positive cells were subsequently gated from the viable cell population. Voltages were set based on autofluorescence of unlabeled cells.

Statistical Analysis

Cell counts were performed in 10 different fields per slide. All experiments were performed in triplicate. The effects of vector treatment and MOI were compared by use of 2-way analysis of variance; however, Tukey tests also were performed, and the data are presented as 2-way analysis of variance with the *P* values from the Tukey tests (*P* < .05).

RESULTS

Generation of AAV Capsids Containing Tet1 Peptide Insertions

We have previously shown that AAV1 can tolerate the insertion of exogenous peptides after VP1 amino acid 590.²⁹ Importantly, we have also shown that the inserted sequences can be displayed

on the surface of assembled AAV particles and can promote novel capsid-protein interactions.^{13,29} To use these findings for the purpose of generating Tet1-modified AAV particles, we introduced oligonucleotides encoding the Tet1 motif into the Cap ORF of the AAV1 helper plasmid pXR1¹⁴ by PCR-based site-directed mutagenesis, creating pXR1-Cap1.D590_P591insTet1a. Short peptide linkers, previously optimized for the display of heterologous ligands,^{11,13} were also included in an attempt to maintain local capsid flexibility and to promote efficient display of the Tet1 epitope on the surface of the assembled AAV vector particles (Table). In the first instance, these were made up of an alanine-serine upstream linker and a glycine-leucine-serine downstream linker flanking the Tet1 epitope (Tet1a designation, Table).

Tet1a-Modified AAV1 Capsid Proteins Inefficiently Package Vector Genomes and Fail to Mediate Efficient Gene Transfer

To assess the impact of the Tet1a modification on DNA packaging and infectivity, we determined particle and infectious titers of AAV1 and Tet1a-modified AAV1, AAV1.D590_P591insTet1a, vectors (Table). A real-time PCR assay was used to assess DRP titer,³⁰ and transduction of HeLa C12 cells was performed to assess particle infectivity. Compared with unmodified AAV1 capsids, the production of AAV1.D590_P591insTet1a capsids was 66.5-fold less efficient ($5.95 \pm 0.41 \times 10^{10}$ DRP per 1 mL for AAV1.D590_P591insTet1a vs $3.96 \pm 2.2 \times 10^{12}$ DRP per 1 mL for AAV1). Similarly, transduction of HeLa C12 cells was significantly impaired by roughly 3 orders of magnitude by the Tet1 modification (see **Figure, Supplemental Digital Content 2**, <http://links.lww.com/NEU/A694>).

Computational Modeling of Tet1-Modified AAV1 Capsid Proteins

We hypothesized that conformational stresses imposed on the AAV1 capsid by the Tet1 peptide insertion might be responsible for the observed decreases in titers. We therefore pursued 2 complementary approaches to rescue titer of peptide-modified AAV1 particles. First, we modeled the structure of the AAV1 capsid at the 3-fold axis of symmetry to see if sequences flanking the Tet1 insert could be altered either to minimize distortion of the native capsid structure or to promote more efficient display of the targeting epitope. Modeling performed with both I-TASSER and SWISS-Model and validated with molecular dynamics simulations in NAMD indicated that the Tet1 peptide favorably forms a pair of antiparallel β strands. Postulating that changing the length of the linker sequences and the linker side chain polarity might predispose this short β sheet motif toward different positioning on the capsid surface, we modeled the structures of 2 additional Tet1 peptide modifications with different linker/scaffolding sequences (Tet1b and Tet1c; Table). When flanked by alanine and serine at the C-terminus and glycine, leucine, and serine at the N-terminus, as in the original Tet1a construct, the Tet1 epitope folded “downward” and packed between and under the VP3 monomer arms that create the 3-fold axis of symmetry. This not only might effectively shield the epitope from any interaction with its targeted receptor but also appeared to distort the native capsid structure at the 3-fold axis of symmetry (Figure 1A). Modification of the C-terminal linker to include aspartic acid and alanine allowed slightly better presentation of Tet1, allowing it to stack alongside the monomer arm into which it was inserted; however, it was still partially buried (Figure 1B). However, the Tet1c modification, which includes additional alanine and aspartic acid residues in the N-terminal linker sequence, allowed the epitope to lie on top of the arm into which it was inserted, resulting in unobstructed display on the capsid surface (Figure 1C). In fact, modeling of the Tet1c modification predicted the presentation of a “looped” version of the Tet1 epitope, with the C-terminal and N-terminal residues of the inserted sequences in close proximity to each other. Insertions such as this, which minimize the induced gap in and therefore might minimize distortion of the native structure, although facilitating more effective presentation of the targeting epitope, could potentially increase both particle titer and the ability of the modified particles to interact with their targeted receptors.

Efficient Production of Mosaic Tet1c-Modified Vectors Capable of Mediating Specific Gene Transfer to Differentiated Pheochromocytoma (PC12) Cells

Based on our computational modeling, we generated 2 additional packaging constructs, pXR1-Cap1.D590_P591insTet1b and pXR1-Cap1.D590_P591insTet1c, for building the modified Tet1b and Tet1c sequences into the AAV1 capsid. As suggested above and described previously by our group,¹³ these constructs were used with AAV helper plasmid pXR1, encoding unmodified

AAV1 capsid proteins, to generate mosaic AAV particles containing different ratios of Tet1-modified and unmodified capsid proteins. Particle titers were determined by real-time PCR, and gene transduction was assessed on HEK 293 and differentiated pheochromocytoma (PC12) cells. Mosaic particles generated from a mixture of 80% Tet1c-modified pXR1 plasmid (pXR1-Cap1.D590_P591insTet1c) and 20% unmodified pXR1 plasmid into HEK 293 packaging cells were produced 4-fold more efficiently than particles made up entirely of Tet1c-modified capsid proteins ($P < .05$), and significant increases in particle titer were realized with the use of optimized linker/scaffolding sequences flanking Tet1 ($P < .05$; Figure 2). These findings validate the ability of particle mosaicism to rescue titer of some tropism-modified AAV vector particles, as well as our computational modeling approach to rationally engineer modified AAV capsids. However, the real benefit of this strategy was evidenced by the ability of Tet1c-modified mosaic AAV1 vectors (Tet1c-rAAV) to mediate significantly enhanced transduction of PC12 cells and significantly lower transduction of HEK 293 cells (Figure 3). Transduction of HEK 293 cells at 100 DRPs per cell decreased >55 -fold from $32.32 \pm 6.98\%$ (mean \pm SEM) to only $0.58 \pm 1.29\%$ ($P < .05$), whereas at 1000 DRPs per cell, transduction decreased from

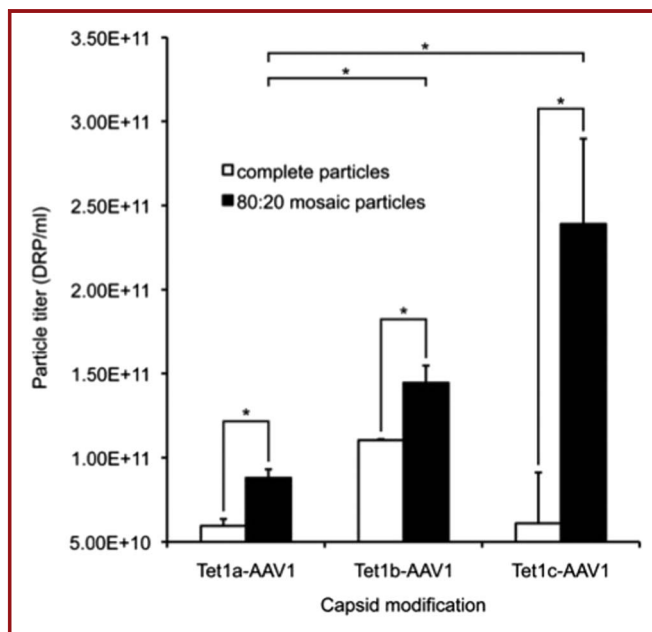
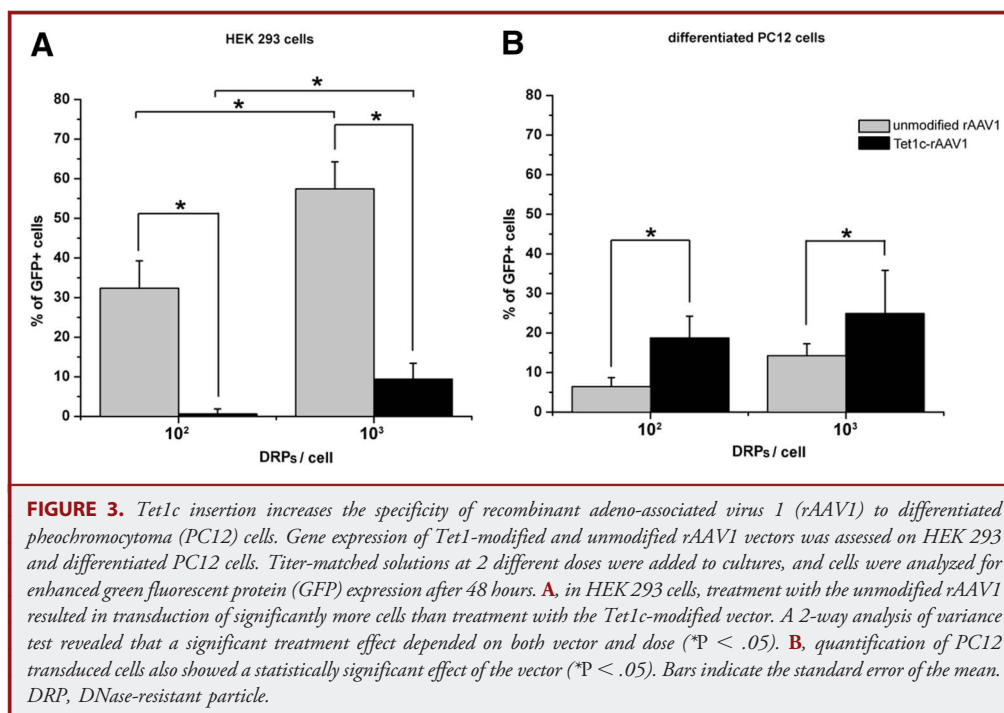


FIGURE 2. Particle titers of Tet1-modified recombinant adeno-associated virus 1 (rAAV1) vectors. DNase-resistant particle (DRP) titers were determined by real-time polymerase chain reaction assay.³⁰ Particles comprising entirely Tet1-modified AAV1 capsid proteins are compared with mosaic particles assembled from HEK 293 cells transfected with an 80:20 mixture of plasmid DNA encoding Tet1-modified AAV1 capsid proteins and unmodified AAV1 capsid proteins. All data are shown as the mean of triplicate determinations. Bars indicate the standard error of the mean. A 2-way analysis of variance test revealed that a significant effect depended on both capsid mosaicism and linker/scaffolding sequences flanking the Tet1 epitope (* $P < .05$).



57.42 ± 6.84% to only 9.39 ± 4.03% ($P < .05$; Figure 3A). Transduction of PC12 cells at 100 DRPs per cell increased from 6.5 ± 2.32% to 18.13 ± 5.51% ($P < .05$) and at 1000 DRPs per cell from 14.21 ± 3.02% to 25.72 ± 10.92% ($P < .05$; Figure 3B). By simultaneously increasing the transduction of PC12 cells while decreasing transduction of nonneuronal HEK 293 cells, a >155-fold ($P < .05$) increase in specificity is realized at the lower MOI, suggesting the utility of these engineered particles. Because axonal uptake and retrograde delivery depend equally on axon terminal affinity (neuronal binding) and available titer (lack of binding to surrounding muscle), increased neuronal specificity is likely more important than affinity alone. Although the technical ease of using immortalized cell lines led us to initially screen *Tet1*-modified vectors on PC12 and HEK 293 cells, having demonstrated increased specificity, we moved on to assess gene transduction in primary spinal cord cultures.

Tet1c-Modified Vectors Mediate Enhanced Gene Transfer to Primary Spinal Neurons

Embryonic day 15 spinal cord cultures (neuron/glia ratio, 8:2) were used to assess gene transduction mediated by *Tet1c*-modified AAV particles. To evaluate the specificity of *Tet1c*-rAAV-mediated gene transfer, cells were stained with antibodies against neuron-specific markers (MAP-2). Figure 4A illustrates an apparent increase in neuronal GFP expression in the *Tet1c*-rAAV treated cultures. At an MOI of 1000 *Tet1c*-rAAV1eGFP DRPs per cell, transgene expression was observed in 61.09 ± 13.23% of spinal cord neurons, whereas only 17.48 ± 7.54% of

spinal cord neurons in these cultures were transduced with unmodified rAAV1eGFP ($P < .05$; Figure 4B).

Tet1c-Modified Vectors Mediate Enhanced Retrograde Axonal Transport to Primary DRG Neurons

It has previously been demonstrated that wild-type AAV undergoes uptake and retrograde transport with limited efficiency.³¹ We hypothesized that modifying AAV using peptides with high affinity for motor neuron receptors might enhance axon terminal uptake. We evaluated retrograde gene delivery using the *Tet1c*-modified AAV1 vector in vitro. Axon terminals of DRG explants plated in Campenot chambers were exposed to *Tet1c*- and unmodified rAAV1 vectors. The percentage of transduced cell bodies in the DRG explants was counted to estimate the tendency of individual vectors to bind axon terminals, to undergo uptake, and to be transported in a retrograde fashion to the cell bodies. We were able to demonstrate that the uptake of *Tet1c*-rAAV1 was markedly enhanced compared with the unmodified vector ($P < .05$; Figure 5). These experiments demonstrate our ability to construct engineered AAV vectors targeted for motor neuron gene delivery.

Tet1c-Modified Vectors Do Not Mediate Enhanced Transduction of C2C12 Cells in Vitro

At an MOI of 10 000, scrAAV1.eCBA.eGFP averaged 76.2% cells transduced and scrAAV1*tet1*.eCBA.eGFP averaged 71.8% cells transduced. At an MOI of 33 000, scrAAV1.eCBA.eGFP averaged 79.3% cells transduced and scrAAV1*tet1*.eCBA.eGFP

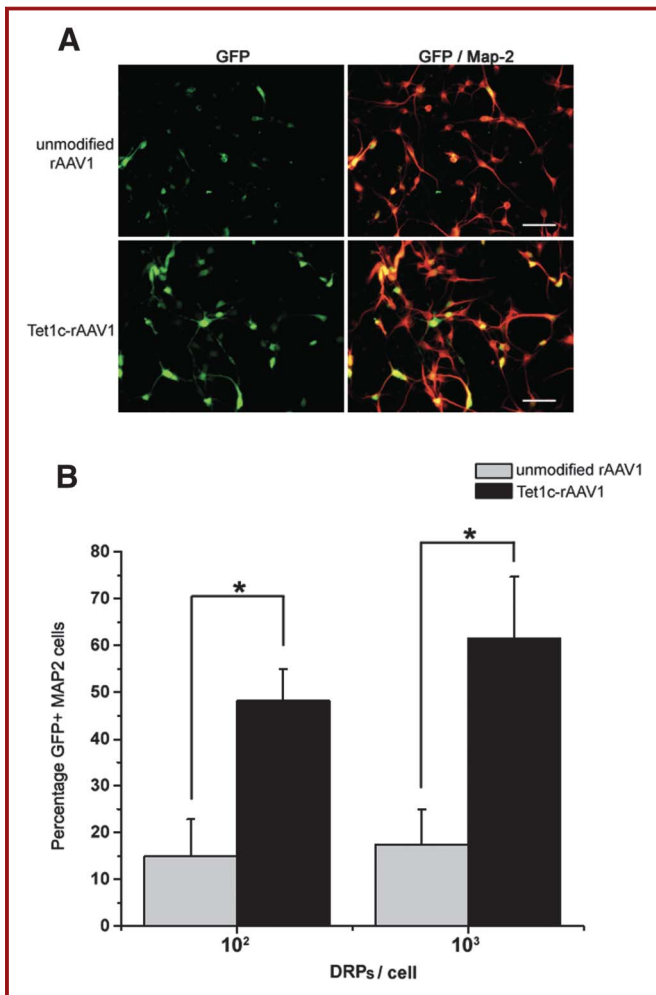


FIGURE 4. *Tet1c* insertion enhances specificity of recombinant adeno-associated virus 1 (rAAV1) to spinal cord neurons. Gene expression of *Tet1*-modified and unmodified rAAV1 vectors was assessed on embryonic day 15 embryonic primary spinal cord cell cultures. Titer-matched solutions at 2 different doses were added to cultures, and cells were analyzed for enhanced green fluorescent protein (GFP) expression after 48 hours. **A**, colocalization of GFP (green) and Map-2 (red) revealed robust neuronal transduction in cultures treated with *Tet1c*-modified rAAV1 particles. Scale bar = 20 μ m. **B**, quantification of transduced neurons in both conditions (unmodified and *Tet1c*-modified groups) confirmed the stronger gene expression observed in *Tet1c*-modified treated spinal cord cells. A 2-way analysis of variance test revealed a significant effect of the vector (* $P < .05$) that was not dependent on dose. DRP, DNase-resistant particle.

averaged 80.6% cells transduced. The difference in mean transduction efficiency at both MOIs did not reach statistical significance ($P = .66$ and $P = .60$, respectively; Figure 6).

DISCUSSION

Since the inception of protein engineering in the early 1980s, the hope has been that the systematic manipulation of viral capsid structure and function can be driven by rational, structure-based

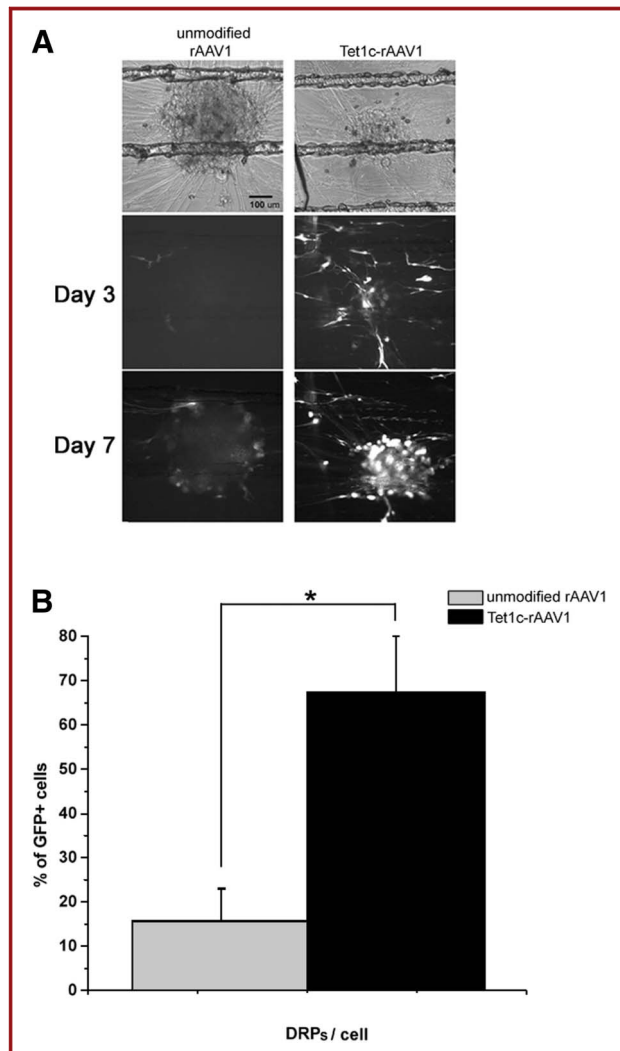
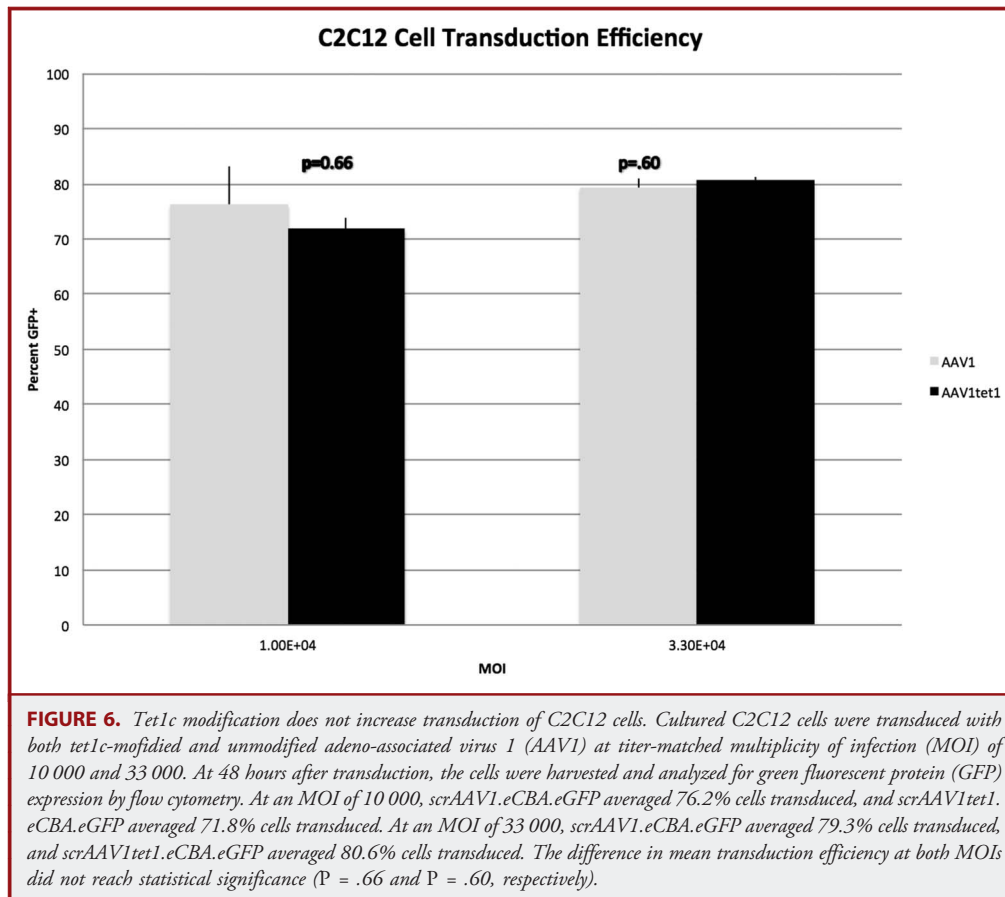


FIGURE 5. *Tet1c* insertion increases retrograde axonal transport in dorsal root ganglia (DRG) neurons. Gene expression of *Tet1*-modified and unmodified recombinant adeno-associated virus 1 (rAAV1) vectors was assessed on embryonic day 15 DRG explants plated in Campenot chambers. Titer-matched solutions were added to the axon terminal compartments, and cell bodies were analyzed for enhanced green fluorescent protein (GFP) expression after 3 and 7 days. **A**, fluorescence images demonstrated a stronger gene expression pattern in DRG neurons treated with the *Tet1c*-modified vector compared with the unmodified rAAV1. Transduced cells colocalized with the contrast-phase images of the explants (top row). Scale bar = 100 μ m. **B**, quantification of transduced DRG cell bodies in both unmodified and *Tet1c*-modified treated chambers revealed a significantly enhanced uptake of *Tet1c*-modified vector as opposed to the unmodified vector (* $P < .05$).

design approaches.³² Over the years, an impressive array of successful experiments have been carried out by applying qualitative rules of protein structure and function through inspection using computer graphics. These include changes in



enzyme substrate specificity,³³ the introduction of metal binding sites into proteins for affinity purification,³⁴ allosteric control,³⁵⁻³⁷ and even the de novo creation of small proteins that adopt defined secondary structures.³⁸ Nevertheless, when applied to large polymeric protein complexes such as virus capsids, these structure-based design approaches rapidly become too complex to solve by visual inspection. One way around this difficulty has been to avoid structure-based design altogether. Recent advances in molecular evolution and library construction have provided sets of experimental tools to generate populations of capsid variants from which vectors with desirable properties can be isolated through the use of various functional screening techniques. Alternatively, through extensive mutational analysis of virus capsid proteins, sites have been identified that are amenable to peptide insertion.^{6,7,9-11} This has allowed the identification of small peptides via robust screening technologies and then their genetic integration into the viral capsid by site-directed mutagenesis. The advantage of the latter approach is that it allows some control over the engineered process because specific cell-surface interactions can be targeted. Currently, much of the research in vector engineering is devoted to the development and application of 1 of these 2 techniques. However, in an increasing number of instances, these techniques

prove insufficient to generate AAV vectors with desired characteristics.

The nature of neurodegenerative diseases, including amyotrophic lateral sclerosis (ALS), has highlighted the necessity for interventional treatments. Targeted therapeutic gene delivery is a promising strategy to decrease the severity and delay the onset of symptoms of these diseases. One of the most promising strategies for targeted gene delivery, genetically modified AAV vectors, has presented certain challenges. Direct injection of the spinal cord carries significant surgical risk and, because of limited vector spread in tissue, is practical only for the treatment of targeted spinal cord segments (cervical or lumbar) rather than the whole cord. In contrast, leveraging the inherent tendency of a variety of vectors to undergo retrograde axonal transport provides a minimally invasive strategy that can be applied to lower motor neuron delivery throughout the whole spinal cord and the even more vulnerable brainstem. Retrograde axonal delivery of vector may provide a useful solution to other challenging problems in neural gene delivery. ALS affects upper and lower motor neurons. These upper motor neurons are distributed widely in the lamina of motor cortex and in a variety of deep brain nuclei. Thus, as with lower motor neuron gene delivery, direct vector injection is impractical for upper motor neuron gene therapy. Similarly, a recently concluded

randomized controlled clinical trial of AAV-mediated gene therapy for Parkinson disease failed to meet the end point of improved motor symptoms.¹ Analysis of postmortem tissue suggested that injection of the putamen (postsynaptic site) failed to deliver sufficient therapeutic transgene to the substantia nigra. These observations led to the design of a current trial that attempts direct injection of this deeper, more vulnerable target. AAV with enhanced neuronal specificity and retrograde transport would provide an alternative, perhaps safer, approach.

Despite its advantages, translation of the retrograde delivery concept has been prevented by difficulty scaling up from rodent models. In ALS models, achieving adequate axonal binding through intramuscular injection requires high titers and volumes of vector, presenting a potential inflammatory risk and biomanufacturing challenges. Recent findings suggest that AAV6 may undergo enhanced retrograde axonal transport after peripheral injection in nonhuman primates, although previous studies in rodents suggest that it is inferior to AAV1.^{31,39} Here, we show that AAV1 vectors can be rationally engineered for targeted gene delivery to motor neurons via enhanced axonal neuronal transport. This same strategy can be used to enhance the axonal affinity and specificity of alternate serotypes that may prove even more effective than AAV1 for retrograde delivery.

CONCLUSION

Genetic modification of the AAV capsid structure is cumbersome, and peptide insertion often results in significantly decreased titer or failure of the engineered insertion to bind to the targeted cell-surface receptor. Because some peptides inserted at a site may prove effective and others inserted at the same site do not, it appears that the primary amino acid sequence of the inserted peptide and the structural context of the insertion site dictate success.^{11,29} Here, we have combined the potential of structure-based design with current peptide targeting strategies to increase the effectiveness of functional capsid engineering. This approach promises a significant advancement in rational structure-based design of AAV-based gene transfer vectors.

We began by modeling the AAV capsid structure and conformation around the 3-fold axis of symmetry using a series of free energy-minimization algorithms. We showed that charge-based interactions between the inserted Tet1 peptide and the surrounding capsid structural environment inhibited effective peptide display and potentially the assembly of intact vector particles. We hypothesized that decreasing this charge difference through the introduction of appropriately charged residues flanking the Tet1 epitope and increasing the flexibility and length on these scaffolding sequences might rescue capsid assembly and peptide display. Rather than building these different modifications into the AAV capsid, generating a series of secondarily modified AAV vectors, and experimentally testing the effectiveness of each modification, we used a novel computational approach to select and prescreen linker sequences for effective peptide display. Through visual and quantitative analysis of the varying

conformations adopted by the capsid and the targeting peptides, we were able to optimize scaffolding sequences for capsid assembly and peptide display. Importantly, our structure-based design approach was verified by experimental analysis.

Disclosure

This work was supported by grants from the National Institutes of Health (R21 AI51388 and RO1 AI51388) to Dr Bartlett and from the ALS Association to Dr Boulis. The authors have no personal, financial, or institutional interest in any of the drugs, materials, or devices described in this article.

REFERENCES

- Marks WJ Jr, Bartus RT, Siffert J, et al. Gene delivery of AAV2-neurturin for Parkinson's disease: a double-blind, randomised, controlled trial. *Lancet Neurol*. 2010;9(12):1164-1172.
- Burger C, Gorbatyuk OS, Velardo MJ, et al. Recombinant AAV viral vectors pseudotyped with viral capsids from serotypes 1, 2, and 5 display differential efficiency and cell tropism after delivery to different regions of the central nervous system. *Mol Ther*. 2004;10(2):302-317.
- Kaspar BK, Llado J, Sherkat N, Rothstein JD, Gage FH. Retrograde viral delivery of IGF-1 prolongs survival in a mouse ALS model. *Science*. 2003;301(5634):839-842.
- Liu JK, Teng Q, Garrity-Moses M, et al. A novel peptide defined through phage display for therapeutic protein and vector neuronal targeting. *Neurobiol Dis*. 2005; 19(3):407-418.
- Federici T, Liu JK, Teng Q, Yang J, Boulis NM. A means for targeting therapeutics to peripheral nervous system neurons with axonal damage. *Neurosurgery*. 2007;60(5):911-918; discussion 911-918.
- Rabinowitz JE, Xiao W, Samulski RJ. Insertional mutagenesis of AAV2 capsid and the production of recombinant virus. *Virology*. 1999;265(2):274-285.
- Girod A, Ried M, Wobus C, et al. Genetic capsid modifications allow efficient re-targeting of adeno-associated virus type 2. *Nat Med*. 1999;5(12):1438.
- Griffman M, Trepel M, Speece P, et al. Incorporation of tumor-targeting peptides into recombinant adeno-associated virus capsids. *Mol Ther*. 2001;3(6):964-975.
- Wu P, Xiao W, Conlon T, et al. Mutational analysis of the adeno-associated virus type 2 (AAV2) capsid gene and construction of AAV2 vectors with altered tropism. *J Virol*. 2000;74(18):8635-8647.
- Shi W, Arnold GS, Bartlett JS. Insertional mutagenesis of the adeno-associated virus type 2 (AAV2) capsid gene and generation of AAV2 vectors targeted to alternative cell-surface receptors. *Hum Gene Ther*. 2001;12(14):1697-1711.
- Shi W, Bartlett JS. RGD inclusion in VP3 provides adeno-associated virus type 2 (AAV2)-based vectors with a heparan sulfate-independent cell entry mechanism. *Mol Ther*. 2003;7(4):515-525.
- Shi W, Hemminki A, Bartlett JS. Capsid modifications overcome low heterogeneous expression of heparan sulfate proteoglycan that limits AAV2-mediated gene transfer and therapeutic efficacy in human ovarian carcinoma. *Gynecol Oncol*. 2006;103(3):1054-1062.
- Stachler MD, Bartlett JS. Mosaic vectors comprised of modified AAV1 capsid proteins for efficient vector purification and targeting to vascular endothelial cells. *Gene Ther*. 2006;13(11):926-931.
- Rabinowitz JE, Rolling F, Li C, et al. Cross-packaging of a single adeno-associated virus (AAV) type 2 vector genome into multiple AAV serotypes enables transduction with broad specificity. *J Virol*. 2002;76(2):791-801.
- Xiao X, Li J, Samulski RJ. Production of high-titer recombinant adeno-associated virus vectors in the absence of helper adenovirus. *J Virol*. 1998;72(3):2224-2232.
- Zolotukhin S, Byrne BJ, Mason E, et al. Recombinant adeno-associated virus purification using novel methods improves infectious titer and yield. *Gene Ther*. 1999;6(6):973-985.
- Okada T, Nonaka-Sarukawa M, Uchibori R, et al. Scalable purification of adeno-associated virus serotype 1 (AAV1) and AAV8 vectors, using dual ion-exchange adsorptive membranes. *Hum Gene Ther*. 2009;20(9):1013-1021.
- Graham FL, Smiley J, Russell WC, Nairn R. Characteristics of a human cell line transformed by DNA from human adenovirus type 5. *J Gen Virol*. 1977;36(1):59-74.
- Clark KR, Voulgaropoulou F, Johnson PR. A stable cell line carrying adenovirus-inducible rep and cap genes allows for infectivity titration of adeno-associated virus vectors. *Gene Ther*. 1996;3(12):1124-1132.

20. Yaffe D, Saxel O. Serial passaging and differentiation of myogenic cells isolated from dystrophic mouse muscle. *Nature*. 1977;270(5639):725-727.
21. Vincent AM, Feldman EL, Song DK, et al. Adeno-associated viral-mediated insulin-like growth factor delivery protects motor neurons in vitro. *Neuromolecular Med*. 2004;6(2-3):79-85.
22. Campenot RB. Development of sympathetic neurons in compartmentalized cultures, II: local control of neurite survival by nerve growth factor. *Dev Biol*. 1982;93(1):13-21.
23. Arnold K, Bordoli L, Kopp J, Schwede T. The SWISS-MODEL workspace: a web-based environment for protein structure homology modelling. *Bioinformatics*. 2006;22(2):195-201.
24. Kiefer F, Arnold K, Kunzli M, Bordoli L, Schwede T. The SWISS-MODEL Repository and associated resources. *Nucleic Acids Res*. 2009;37(database issue):D387-D392.
25. Wu S, Skolnick J, Zhang Y. Ab initio modeling of small proteins by iterative TASSER simulations. *BMC Biol*. 2007;5:17.
26. Zhang Y. Template-based modeling and free modeling by I-TASSER in CASP7. *Proteins*. 2007;69(suppl 8):108-117.
27. Zhang Y. I-TASSER server for protein 3D structure prediction. *BMC Bioinformatics*. 2008;9:40.
28. Phillips JC, Braun R, Wang W, et al. Scalable molecular dynamics with NAMD. *J Comput Chem*. 2005;26(16):1781-1802.
29. Arnold GS, Sasser AK, Stachler MD, Bartlett JS. Metabolic biotinylation provides a unique platform for the purification and targeting of multiple AAV vector serotypes. *Mol Ther*. 2006;14(1):97-106.
30. Clark KR, Liu X, McGrath JP, Johnson PR. Highly purified recombinant adeno-associated virus vectors are biologically active and free of detectable helper and wild-type viruses. *Hum Gene Ther*. 1999;10(6):1031-1039.
31. Hollis ER II, Kadoya K, Hirsch M, Samulski RJ, Tuszynski MH. Efficient retrograde neuronal transduction utilizing self-complementary AAV1. *Mol Ther*. 2008;16(2):296-301.
32. Hellinga HW. Computational protein engineering. *Nat Struct Biol*. 1998;5(7):525-527.
33. Wilks HM, Holbrook JJ. Alteration of enzyme specificity and catalysis by protein engineering. *Curr Opin Biotechnol*. 1991;2(4):561-567.
34. Arnold FH, Haymore BL. Engineered metal-binding proteins: purification to protein folding. *Science*. 1991;252(5014):1796-1797.
35. Higaki JN, Haymore BL, Chen S, Fletterick RJ, Craik CS. Regulation of serine protease activity by an engineered metal switch. *Biochemistry*. 1990;29(37):8582-8586.
36. Browner MF, Hackos D, Fletterick R. Identification of the molecular trigger for allosteric activation in glycogen phosphorylase. *Nat Struct Biol*. 1994;1(5):327-333.
37. Brinen LS, Willett WS, Craik CS, Fletterick RJ. X-ray structures of a designed binding site in trypsin show metal-dependent geometry. *Biochemistry*. 1996;35(19):5999-6009.
38. Bryson JW, Betz SF, Lu HS, et al. Protein design: a hierarchic approach. *Science*. 1995;270(5238):935-941.
39. Towne C, Schneider BL, Kieran D, Redmond DE Jr, Aebischer P. Efficient transduction of non-human primate motor neurons after intramuscular delivery of recombinant AAV serotype 6. *Gene Ther*. 2010;17(1):141-146.

Supplemental digital content is available for this article. Direct URL citations appear in the printed text and are provided in the HTML and PDF versions of this article on the journal's Web site (www.neurosurgery-online.com).

COMMENT

This work demonstrates the utility of structure-based design of viral vectors in order to modify viral tropism. The generation of targeted viral vectors is a powerful technique in the advance of gene therapy.

Edmund Hollis II
La Jolla, California



NEUROSURGERY Video Content Record. View. Experience.

As an archive of technique videos and tutorials published with previous *Neurosurgery* and *Operative Neurosurgery* articles, the Video Gallery is your resource for cutting-edge surgical demonstrations.
Find it at neurosurgery-online.com.

Videos are also offered free on *Neurosurgery's* YouTube page
youtube.com/neurosurgeryens.

NEUROSURGERY